Effects of μPDE-Driven Excitation on a Model Supersonic Combustor

Keon-Hyeong Lee, Bu-Kyeng Sung, Su-Wan Choi, Gyeong-Ui Mo, Jeong-Yeol Choi*
Department of Aerospace Engineering, Pusan National University
Busan, 46241, Republic of Korea

1 Introduction

For hypersonic flight, a wide range of concepts have been considered such as RBCC, shock-induced combustion, and the supersonic pulse detonation engine [1-7]. Among these, the scramjet engine is considered a key technology. However, scramjet vehicles face several major challenges that must be overcome. One of the main challenges is that the scramjet engine intakes air at supersonic speeds. As a result, the flow residence time is generally within 1 ms. In contrast, the chemical reaction time varies from 10^{-10} sec to 1 sec, depending on initial conditions [8]. Achieving fuel-air mixing, stable ignition, and flame holding within this short time is essential. To address these issues, ideas are being proposed from various perspectives [9]. Recent methods for improving scramjet combustion efficiency can be divided into passive and active methods. Passive methods include utilizing structures such as cavities and struts, while active methods consider pulse jets, plasma, and detonation. The cavity creates a recirculation zone, increasing flow residence time and providing favorable conditions for flame stabilization [10]. Among active methods, techniques such as using pulse jets or plasma are being studied to enhance combustion efficiency. However, these methods may require high-pressure gas sub-tank or large electrical energy. Therefore, some researchers have conducted studies on delivering detonation into the supersonic combustor. Ombrello et al [11]. conducted an experimental investigation on transmitting detonation into a supersonic flow using a pulse detonator (PD). As a result, the detonation plume provides localized blockage effect and enhances near-field mixing.

The goal of this study is to generate detonation using a micro-Pulse Detonation Engine (μPDE) and investigate its effects on the supersonic combustor when transmitted into it. Additionally, this study explores the potential of using a μPDE to improve the supersonic combustion efficiency. To achieve this, experiments were conducted using the Pusan Nat'l Univ. Direct-Connect Supersonic Combustor (PNU-DCSC). In these experiments, the μPDE was used as an active excitation device, while the cavity served as a flameholder and a passive excitation device.

2 Experimental Apparatus

The configuration of the PNU-DCSC is shown in Fig. 1. This device consists of a total of four sections: Vitiation Air Heater (VAH), Circular to Rectangular Shape Transition (CRST) nozzle, isolator, supersonic combustor. The VAH generates high-enthalpy vitiated air using gaseous hydrogen, oxygen,

Correspondence to: aerochoi@pusan.ac.kr

and air. The VAH supplies a total mass flow rate of 368 g/s. Through the combustion, the VAH generates vitiated air with a total pressure of 1.69 MPa and a total temperature of 1,600 K. The vitiated air is accelerated to Mach 2 through the CRST nozzle and supplied to the isolator inlet. These conditions have been validated through numerical analysis and experimental investigation [12-15].

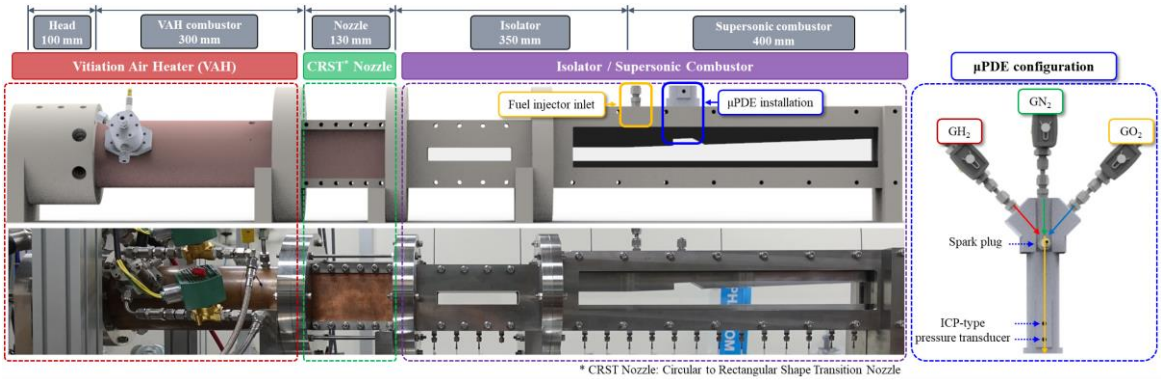

Figure 1: Configuration of Direct-Connect Supersonic Combustor at Pusan National University.

The schematic of the isolator and the supersonic combustor are detailed in Fig. 2. The isolator has a cross-section of 20 × 20 mm^2 and a length of 350 mm. The supersonic combustor has a length of 400 mm and a divergence angle of 2º. The supersonic combustor uses gaseous hydrogen as fuel. Also, the fuel injector was designed as a 30º inclined injector. The cavity is located 70 mm from the starting point of the supersonic combustor. The cavity has a depth of 10 mm, a bottom wall length of 30 mm, and a ramp angle of 30º. Due to the ramp angle, the length to depth ratio (L/D) is 3.86. The μPDE uses gaseous hydrogen and oxygen as fuel and oxidizer, respectively, and gaseous nitrogen as a purge gas. The μPDE has an inner diameter of 4.22 mm, and its exit is located at the center of the bottom of the cavity.

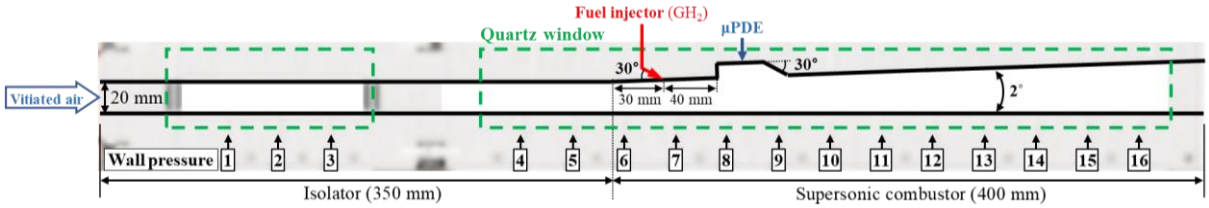

Figure 2: Schematic of isolator-supersonic combustor.

For high-speed visualization, a Z-type Schlieren system and a Phantom v2512 high-speed camera were used. The high-speed camera images were recorded at 110,000 fps with a resolution of 1,024 × 208. For wall pressure measurements, the 16 channels Scanivalve DSA3217 was used. To measure the detonation velocity propagating within the μPDE, two PCB ICP-type 113B-series dynamic pressure sensors were used. The LabVIEW software was used for measurement and control.

Combustion experiments followed the sequence shown in Fig. 3.: (1) GH_2 and GO_2 are supplied into the VAH. (2) The VAH is ignited by the CWI, and the VAH pressure rises. Simultaneously, air is supplied into the VAH. (3) GH_2 fuel is injected into the supersonic combustor according to the set pressure. (4) The μPDE operates according to the set sequence, where detonations are periodically formed within the μPDE and subsequently transmitted and expanded into the supersonic combustor in the form of blast waves. The supersonic combustor ignites during the first operation of the μPDE, and the ignition process of the supersonic combustor can be understood by referring to previous study [16]. (5) All valves close, and the experiment ends.

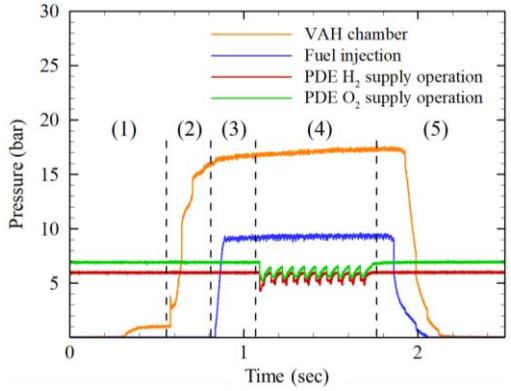

Figure 3: The experimental sequence and pressure history.

3 Experimental Results

The experimental conditions for each case are presented in Table 1. Each case was classified based on the fuel injection pressure (P_{inject}) and the operating frequency of the μPDE. The fuel/oxidizer supply pressures for the μPDE were adjusted according to the supersonic combustion pressure. In Case 25-20, despite supplying GH_2 and GO_2 to the μPDE at a pressure near the maximum allowed by the solenoid valve, detonation formation within the μPDE failed.

Table 1: Summary of representative experimental conditions and results.

Case	P_{inject}	$Ø_{global}$	μPDE operation	μPDE supply condition (GH_2-GO_2)	DDT
10-10	10 bar	0.110 ± 0.009	10 Hz	6 bar – 7 bar	Success
10-20			20 Hz		
15-10	15 bar	0.168 ± 0.005	10 Hz		
15-20			20 Hz		
25-10	25 bar	0.291 ± 0.010	10 Hz	9 bar – 10 bar	Success
25-20			20 Hz	10 bar – 11 bar	Fail

The bottom wall pressure distribution along the isolator and supersonic combustor is shown in Fig. 4. The 'Single Shot' label indicates the wall pressure when no active excitation was performed. The pressures indicated by the blue and green lines represent the bottom wall pressure before the start of the next μPDE cycle. Even before the μPDE was operated, the supersonic combustion pressure near the cavity was measured to be higher than when no excitation was performed. Additionally, the pressure was measured to be higher at 20 Hz active excitation case compared to 10 Hz. As a result, it was confirmed that the excitation effect occurs even with low-frequency excitation of 10-20 Hz. In Case 25-20, the supersonic combustion pressure was measured to be lower than that of the 10 Hz active excitation case because detonation failed to form within the μPDE. The failure of the Deflagration-to-Detonation Transition (DDT) process in the μPDE is thought to be due to an insufficient supply pressure to the μPDE. Although the supersonic combustion pressure increased with the rise in equivalence ratio, the fuel and oxidizer supply pressure for the μPDE was insufficient. As the supersonic combustion pressure increases, it is expected that increasing the supply pressure in the μPDE could induce the DDT process. However, this could not be performed due to the solenoid valve operating limits.

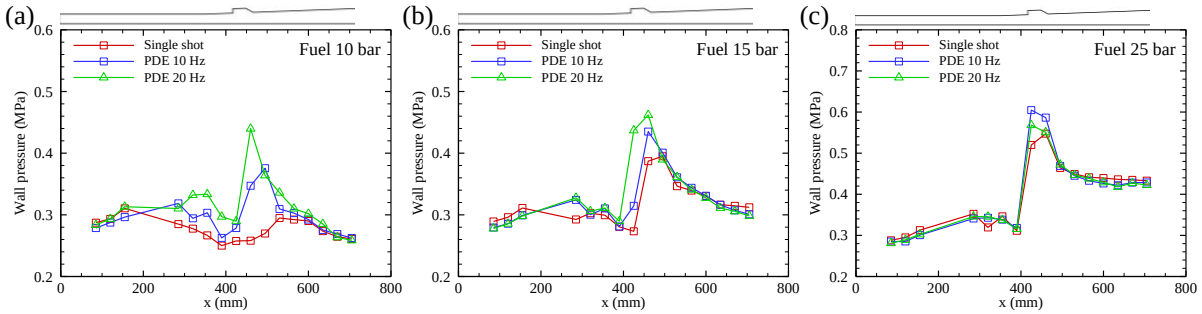

Figure 4: Bottom wall pressure distribution along the isolator and supersonic combustor.

Fig. 5 (a) shows the location of the pixel data (red line) used to create the x-t-Schlieren diagrams. Fig. 5 (b)~(d) shows, from left to right, Schlieren snapshots captured when the μPDE is ignited; an x-t-p diagram displaying wall pressure variations over the entire experimental period; and an x-t-Schlieren diagram based on Schlieren snapshots illustrating changes within the supersonic combustor over one cycle of μPDE operation.

To illustrate the flow changes inside the supersonic combustor resulting from μPDE operation, Schlieren images were sequentially presented in the left side of Fig. 5 for each case. Cases 10-10 to 15-10 were grouped together because they show similar flow field changes and flame structures. Roman numerals are used to label the sequence as follows: (I) Before the μPDE ignition, the flame was stabilized. (Case 10-10 to 15-20: cavity shear layer flame, Case 25-10: cavity flame). (II) The mixture began to charge into the μPDE, and an overfilled mixture flowed into the supersonic combustor, increasing the flame area. (III) The μPDE was ignited, and after detonation was formed via DDT within the μPDE, it propagated into the supersonic combustor in the form of a blast wave. (IV) After the blast wave exhaust, the shock train momentarily moved upstream, altering the flame structure (Case 10-10 to 15-20: cavity flame, Case 25-10: cavity-assisted jet wake flame). In the Case 25-20, since the DDT process in the μPDE failed, Schlieren images are not presented. While the processes in (I) and (II) are the same for Case 25-20, the process in (III) did not occur.

The x-t-p diagram in the center of Fig. 5 shows changes in the bottom wall pressure within the supersonic combustor over the entire experimental period. The supersonic combustor is ignited by the μPDE, causing a pressure increase, and high pressure is continuously maintained with the periodic operation of the μPDE. In particular, it can be observed that high pressure persists around and slightly downstream of the cavity. When the blast wave is transmitted into the supersonic combustor after μPDE ignition, it can also be observed that the pressure momentarily increases up to the leading edge of the cavity.

The x-t-Schlieren diagram in the right of Fig. 5 shows shock position changes within the supersonic combustor during one cycle of μPDE operation. It can be observed that a shock at the front moves upstream following the operation of the μPDE. However, the shock only weakly propagates upstream and does not reach as far as the isolator. It can be inferred that, despite the strong blast wave being directly transmitted from the μPDE, it does not exert a destructive impact as far as the isolator.

Previously, it was believed that high-frequency excitation over 100 Hz was necessary to induce flow excitation in a supersonic combustor. However, when considering various factors such as thermal management, maintaining the operational mode, and protecting thermal coatings and structural components, low-frequency operation of the μPDE may offer greater advantages. Furthermore, based on Schlieren snapshots, instantaneous thermal choking appears to occur after μPDE ignition. Simultaneously, as the equivalence ratio increases, the flow recovery time after μPDE operation becomes longer. As a result, high-frequency operation of the μPDE may lead to excessive heat addition, potentially inducing an unintended early transition in the combustion mode. Although further investigation into the effects of high-frequency excitation is required, operating the μPDE at 10–20 Hz may contribute to improving overall combustion efficiency in scram mode.

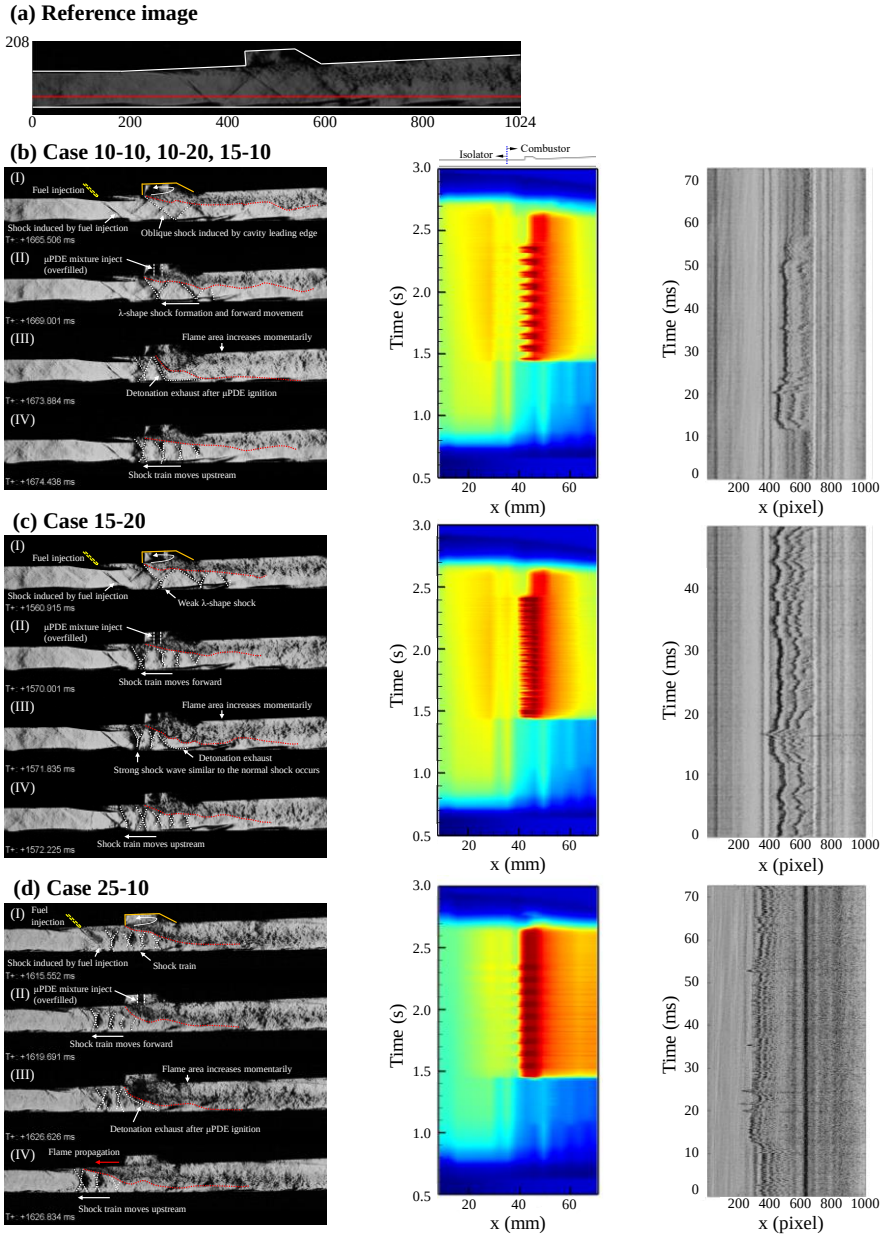

Figure 5: (Left to right) Schlieren snapshots, x-t-p diagram, x-t-Schlieren diagram: (a) The pixel data position used when creating the x-t-Schlieren diagram (red line); (b) Case 10-20 (Similar flow field behavior is also observed in Case 10-10 and Case 15-10); (c) Case 15-20; (d) Case 25-10.

4 Conclusions

In this study, combustion experiments in the supersonic combustor were conducted using both the passive excitation method of a cavity and the active excitation method of the μPDE. When the equivalence ratio of the supersonic combustor was 0.110 and 0.168, the supersonic combustor operated in scram mode, and the μPDE effectively provided excitation effect even at a low operation frequency of 10-20 Hz. However, as the equivalence ratio of the combustor increased, the supersonic combustion pressure also rose, resulting in the μPDE not operating effectively. If the μPDE supply pressure can be actively controlled according to the supersonic combustion pressure, it is expected that the combustion efficiency of the supersonic combustor could be improved in the future.

References

[1] Choi JY, Jeung IS, Yoon Y. (1999). Unsteady-State Simulation of Model Ram Accelerator in Expansion Tube. AIAA journal 37(5): 537–543.

[2] Kim SL, Choi JY, Jeung IS, Park YH. (2001). Application of approximate chemical Jacobians for constant volume reaction and shock-induced combustion. Applied Numerical Math. 39(1): 87−104.

[3] Kim HS, Oh S, Choi JY. (2017). Quasi-1D analysis and performance estimation of a sub-scale RBCC engine with chemical equilibrium. Aerosp. Sci. Tech. 69: 39–47.

[4] Choi JY, Jeung IS, Yoon Y. (1998). Scaling effect of the combustion induced by shock-wave boundary-layer interaction in premixed gas. Symposium (International) on Combustion 27(2): 2181–2188.

[5] Ma F, Choi JY, Yang V. (2005). Thrust Chamber Dynamics and Propulsive Performance of Single-Tube Pulse Detonation Engines. J. Prop. Pow. 21(3): 512–526.

[6] Choi JY, Ma F, Yang V. (2005). Dynamics Combustion Characteristics in Scramjet Combustors with Transverse Fuel Injection. 41st AIAA/ASME/SAE/ASEE Joint Propulsion Conference and Exhibit, Tucson, AZ, AIAA 2005-4428.

[7] Choi JY, Noh J, Byun JR, Lim JS, Togai K, Yang V. (2011). Numerical Investigation of Combustion/Shock-train Interactions in a Dual-Mode Scramjet Engine. 17th AIAA International Space Planes and Hypersonic Systems and Technologies Conference, San Francisco, CA, AIAA 2011-2395.

[8] Segal C. (2009). The Scramjet Engine: Processes and Characteristics. 1st ed. Cambridge University Press, NY: 128.

[9] Liu Q, Baccarella D, Lee T. (2020). Review of combustion stabilization for hypersonic airbreathing propulsion. Prog. Aerosp. Sci. 119: 100636.

[10] Ben-Yaker A, Hanson RK. (2001). Cavity Flame-Holders for Ignition and Flame Stabilization in Scramjets: An Overview. J. Prop. pow. 17(4): 869-877.

[11] Ombrello T, Carter C, McCall J, Schauer F, Naples A, Hoke J, Hsu KY. (2015). Enhanced Mixing in Supersonic Flow Using a Pulse Detonator. J. Prop. Pow. 31(2): 654-663.

[12] Sung BK, Jeong SM, Choi JY. (2023). Direct-connect supersonic nozzle design considering the effect of combustion. Aerosp. Sci. Tech. 113: 108094.

[13] Lee JH, Lee ES, Han HS, Kim MS, Choi JY. (2023). A Study on a Vitiated Air Heater for a Direct-Connect Scramjet Combustor and Preliminary Test on the Scramjet Combustor Ignition. Aerospace 10(5): 415.

[14] Sung BK, Hwang WS, Choi JY. (2020). Design of a Shape Transition Nozzle for Lab-scale Supersonic Combustion Experimental Equipment. J. Korean Soc. Aeronaut. Space Sci. 48(3): 207–215.

[15] Sung BK, Choi JY. (2021). Design of a Mach 2 shape transition nozzle for lab-scale direct-connect supersonic combustor. Aerosp. Sci. Tech 117: 106906.

[16] Kim MS, Koo IH, Lee KH, Lee ES, Han HS, Jeong SM, Kim H, Choi JY. (2023). Experimental Study on the Ignition Characteristics of Scramjet Combustor with Tandem Cavities Using Micro-Pulse Detonation Engine. Aerospace 10(8):10080706.